JACS
JOURNAL OF THE AMERICAN CHEMICAL SOCIETY

COMMUNICATION

pubs.acs.org/JACS

Reversible Redox of NADH and NAD$^+$ at a Hybrid Lipid Bilayer Membrane Using Ubiquinone

Wei Ma,[†] Da-Wei Li,[†] Todd C. Sutherland,[‡] Yang Li,[†] Yi-Tao Long,*[,†] and Hong-Yuan Chen[§]

[†]Shanghai Key Laboratory of Functional Materials Chemistry and Department of Chemistry, East China University of Science and Technology, 130 Meilong Road, Shanghai 200237, P.R. China

[‡]Department of Chemistry, University of Calgary, 2500 University Drive NW, Calgary, Canada T2N1N4

[§]Key Laboratory of Analytical Chemistry for Life Science and Department of Chemistry, Nanjing University, 22 Hankou Road, Nanjing 210093, P.R. China

Supporting Information

ABSTRACT: Here, we report the reversible interconversion between NADH and NAD$^+$ at a low overpotential, which is in part mediated by ubiquinone embedded in a biomimetic membrane to mimic the initial stages of respiration. This system can be used as a platform to examine biologically relevant electroactive molecules embedded in a natural membrane environment and provide new insights into the mechanism of biological redox cycling.

During the initial stages of respiration, nicotinamide adenine dinucleotide (NADH):ubiquinone oxidoreductase (complex I) catalyzes a two-electron transfer from NADH to ubiquinone, coupled to a transmembrane four-proton translocation, helping to provide the proton-motive force required for the synthesis of adenosine triphosphate.[1] The well-known 'Q cycle' model in mitochondria is based on the tight coupling of both NADH and ubiquinone.[2]

Although the interactions between NADH and ubiquinone have been studied extensively in biological systems, a biomimetic model system has been elusive because of the inherent complexity. Recent insight into the structures of electrode-supported hybrid bilayer membranes (HBMs) has provided a platform to investigate biological applications.[3−6] A typical HBM system consists of a phospholipid layer physisorbed to a self-assembled monolayer (SAM) of alkanethiols that are covalently attached to a gold substrate. The polar head groups of the phospholipids are orientated away from the gold surface to the aqueous solution, and the hydrophobic tails orient toward the hydrophobic SAM.[7−10] The alkylthiols typically form a complete hydrophobic layer at the gold substrate and provide the driving force for the formation of HBM.[8] Although HBM strategies are diverse and well-established, there are very few examples of embedding redox-active molecules in a HBM system.[11−13] When redox molecules self-assemble onto the surface of a gold substrate, a HBM is easily formed by the adsorption of lipid vesicles to produce a supported hybrid lipid bilayer, as illustrated in Scheme 1. The HBM environment resembles the biological membrane, which can dramatically affect the properties of the embedded redox molecule.[13]

Unlike most redox molecules, ubiquinone, also known as coenzyme Q, is composed of the redox active quinoid moiety possessing a tail of long isoprenoid units and is found at the hydrophobic core of the phospholipid bilayer of the inner membrane of mitochondria.[14] As an essential cofactor, ubiquinone also serves as a mobile carrier, transferring electrons and protons in the respiratory chain,[15] generating interest as a system to clarify electron-/proton-transfer processes. On the other hand, the NADH/NAD$^+$ coenzyme couple is one of the most important redox mediators and functions as biology's reducing agent.[16] The electrochemical oxidation of NADH to enzymatically active NAD$^+$ has attracted attention because NADH participates in a variety of enzymatic reactions, including more than 300 dehydrogenases.[17] Interestingly, the direct electrochemical oxidation of NADH at conventional electrodes is both electrochemically irreversible and requires high overpotentials.[16] This overpotential was overcome by using redox mediators, such as quinones.[19−21] The interaction between the mediator and NADH oxidation has been explained in terms of a hydride transfer mechanism in which the mediator accepts a hydride.[22]

To our knowledge, despite extensive efforts to overcome the NADH overpotential with redox mediators, reversible electrochemical interconversion between NADH and NAD$^+$ to mimic the reactions present in the respiratory chain has not been reported. The only reported study that shows the reversible interconversion between NADH and NAD$^+$ without application of an overpotential is mediated by complex I.[23] Furthermore, the redox wave for the NADH/NAD$^+$ complex I-mediated redox couple is sigmoidal, has a large peak-to-peak separation, and was carried out in an aqueous solution, not in a biomimetic membrane environment.

Herein, we report a biomimetic membrane model in which ubiquinone is embedded in a HBM that contains the NADH/NAD$^+$ redox couple ($\mathbf{Q}_n\mathbf{S}$-HBM-NADH/NAD$^+$) as shown in Scheme 1. The findings represent the first report of reversible NADH/NAD$^+$ interconversion caused by a ubiquinone mediator in a biomimetic membrane model. The first step to form the membrane model is the modification of a gold electrode surface with a disulfide derivative of ubiquinone using SAM techniques. Three ubiquinone-terminated disulfides with different alkyl spacers ($\mathbf{Q}_n\mathbf{S}$, n = 1, 5, and 10, respectively)[24] were synthesized and used to modify the gold electrodes (Supporting Information [SI]), assess monolayer stability, and modulate the kinetics of charge transfer. After SAM formation, the ubiquinone-modified gold electrode was then incubated in a vesicle solution, which is

Received: May 2, 2011
Published: July 20, 2011

Scheme 1. Structures of Three Ubiquinone-Terminated Disulfides (Q_nS) and Schematic of Biomimetic Membrane Containing Ubiquinones and NADH/NAD$^+$ Redox Systems (Q_nS-HBM-NADH/NAD$^+$)

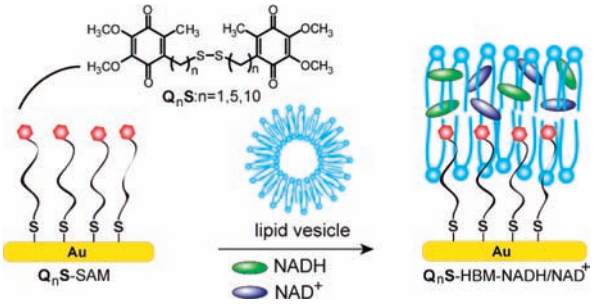

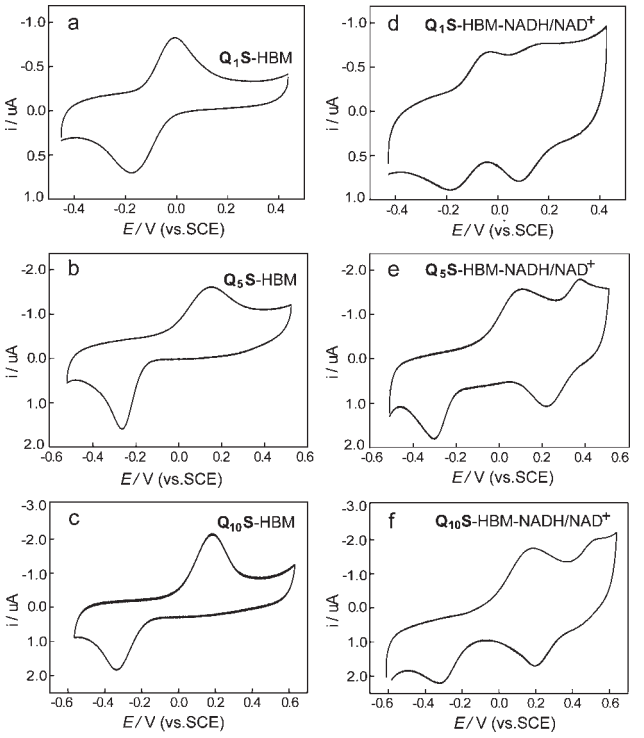

Figure 1. CVs at 100 mV·s^{-1} of the ubiquinone HBM system in the absence (a−c) and presence (d−f) of embedded NADH/NAD$^+$. Q_1S-embedded HBM system (a and d), Q_5S-embedded HBM system (b and e), and $Q_{10}S$-embedded HBM system (c and f) .

known to form suspended lipid bilayers by fusion with the surface of SAM-modified gold electrode.[7−10] A subset of vesicles also contained embedded NADH/NAD$^+$ following established procedures of Fainstein[25] and Bourdillon.[26] This approach to supported bilayer formation allows for control of the ubiquinone electron transfer rate (by tether length modification) and investigations into communication between ubiquinone and the NADH/NAD$^+$ redox couple in a biologically relevant medium.

HBMs were characterized with electrochemical impedance spectroscopy (EIS), high-resolution X-ray photoelectron spectroscopy (XPS), and tapping-mode atomic force microscopy (TM-AFM). The observed capacitance changes in EIS (Figure S22, SI) of the electrode after exposure to the lipid vesicle solution is consistent with the formation of a HBM and indicates that NADH/NAD$^+$ do not induce large defects in the HBM. The high-resolution XPS spectra (Figure S23, SI) and TM-AFM images (Figure S24, SI) also confirmed the formation of HBM layers and the inclusion of NADH/NAD$^+$. Panels a−c of Figure 1 show cyclic voltammetry (CV) redox waves associated with the 2e$^-$, 2H$^+$ redox reaction of ubiquinones (Q_1S, Q_5S, and $Q_{10}S$) that are embedded in the HBM without NADH/NAD$^+$ coenzyme in 0.1 M phosphate buffer solution (PBS, pH 7.0) at a scan rate of 100 mV·s^{-1}. Note the resulting CV waves are consistent with water being present in the HBM. The formal redox potentials of Q_1S, Q_5S, and $Q_{10}S$ experience slight changes of −0.11, −0.10, and −0.08 V, respectively, perhaps attributed to the bilayer depth penetration. The formal redox potentials of Q_nS in the HBMs are in agreement with reported values of ubiquinone at −0.13 V vs SCE of pH 7.0 (Table S2, SI). The three ubiquinones, Q_nS-HBM, of Figure 1a−c qualitatively show an increase in peak separation, indicating a slowing of charge transfer rate with increasing alkyl chain lengths. The slower charge transfer kinetics associated with longer alkyl chains is commonly observed in SAMs of redox-active molecules[27] and is consistent with an electron transfer process that is forced to proceed at a larger distances between ubiquinone and electrode surface. A quantitative kinetic analysis, using Laviron's formalism, is carried out in the SI (Figures S25−S26), and the results are consistent with a two-electron, two-proton transfer process[28] for surface-confined quinone monolayers. On the basis of the peak-to-peak separation between the oxidation and reduction waves, the voltammetric responses range from quasi-reversible for Q_1S-HBM to irreversible for Q_5S-HBM and $Q_{10}S$-HBM.

Panels d−f in Figure 1 show the same Q_nS-HBMs that now contain the lipid-embedded NADH/NAD$^+$. The ubiquinone in the HBM still undergoes similar redox chemistry as described above; however, a second redox event is evident after NADH/NAD$^+$ has been immobilized in the HBMs (Q_1S-HBM-NADH/NAD$^+$, Q_5S-HBM-NADH/NAD$^+$, and $Q_{10}S$-HBM-NADH/NAD$^+$, respectively). Importantly, the new redox couple is ascribed to the reversible NADH/NAD$^+$ redox reaction at a low overpotential. The role of the lipid bilayer in the reversible NADH/NAD$^+$ redox reaction was confirmed by forming a Q_nS-HBMs system that does not contain NADH/NAD$^+$ in the lipid membrane, and instead NADH/NAD$^+$ was added to the electrolyte. With NADH/NAD$^+$ in solution (not embedded in the bilayer membrane) CV experiments were conducted to probe the reversible nature of the NADH/NAD$^+$ redox reaction; reversible redox peaks were not observed, and NADH was only irreversibly oxidized at a potential of ∼0.60 V vs SCE (Figure S27, SI). Lipid confinement of NADH/NAD$^+$ plays two critical roles: (1) higher localized concentration, thus more collisional probability between ubiquinone and NADH/NAD$^+$; (2) the hydrophobic environment of lipid favors communication between ubiquinone and NADH/NAD$^+$. To confirm that reversible NADH/NAD$^+$ interconversion was mediated by surface-confined ubiquinone rather than lipid confinement only, a control experiment in which Q_nS was replaced by an alkylthiol monolayer (Figure S28, SI) in a NADH/NAD$^+$ embedded HBM was conducted and resulted in irreversible oxidation of NADH at a potential (∼0.60 V vs SCE). We propose that the surface-attached ubiquinone acts as an efficient mediator to enhance the heterogeneous proton-coupled electron transfer reaction in the oxidation reaction of NADH to NAD$^+$. The reverse reduction reaction of NAD$^+$ to NADH conversion is unlikely mediated by ubiquinone due to the difference in

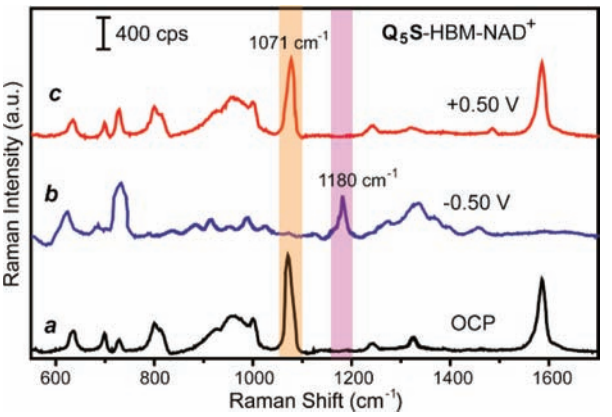

Figure 2. SERS spectra of $\mathbf{Q_5S}$-HBM with embedded NAD^+ on SERS-active rough gold mesh substrates ($\mathbf{Q_5S}$-HBM-NAD^+) as a function of applied potential measured using a 785-nm laser at 10 mW with 20 s of acquisition time. (a) Open circuit potential (OCP); (b) applied potential of −0.50 V vs Ag/AgCl; (c) applied potential of +0.50 V vs Ag/AgCl.

reduction peak potentials in CVs d−f in Figure 1. Further, the observed NADH/NAD^+ formal potential in the HBMs is shifted compared those in the literature at −0.56 V vs SCE of pH 7.0 (Table S2, SI) and may reflect a higher proton concentration in the HBM than in the bulk solution. Cumulatively, these experiments suggest that reversible interconversion between NADH and NAD^+ occurs at a low overpotential when both ubiquinone and NADH/NAD^+ are immobilized in lipid bilayers.

Interestingly, the CV experiments of the reversible NADH and NAD^+ redox reaction show a kinetic difference, as assessed by the peak separation that parallels the kinetics of the ubiquinone charge transfer reaction. The change in the rate of NADH/NAD^+ reaction could result from a specific interaction between ubiquinone and either nicotinamide or adenine. Alternatively, the NADH/NAD^+ may not have easy access to the gold surface with the more tightly packing, longer alkyl chains and the greater distance in the $\mathbf{Q_{10}S}$ monolayer. The kinetics of the NADH/NAD^+ redox reaction further highlights the important role that the ubiquinone and lipid membrane must play in mediating the charge transfer reaction.

Surface enhanced Raman scattering (SERS) is a tool to monitor electrochemical phenomena even down to single molecule levels[29] and optical modulation[30,31] was used here to monitor the reversible electrochemical interconversion between NADH and NAD^+ in the biomimetic membrane model.

In situ SERS spectroelectrochemical experiments were used to monitor NAD^+ and NADH by electrochemical modulation. To clearly elucidate the interconversion between NAD^+ and NADH, only NAD^+ was immobilized in the lipid bilayer for SERS study, and Figure 2 shows the SERS spectra obtained under different potentials. The spectra were acquired as a function of the applied potential in 0.1 M PBS (pH 7.0) on a $\mathbf{Q_5S}$-HBM-NAD^+ SERS-active gold mesh substrate. The potential was scanned from open circuit potential to −0.5 V then to +0.50 V, such that NAD^+ evolves from its oxidized state (NAD^+), to being fully reduced (NADH) and returns to its oxidized form (NAD^+). The nicotinamide ring structures of NAD^+ and NADH have unique spectroscopic signatures and yield Raman spectral changes in intensity and peak position. An initial spectrum of NAD^+ acquired before an applied voltage is shown as Figure 2, curve a. Under open circuit conditions, a significant signal from the intense SERS band of $\mathbf{Q_5S}$-HBM-NAD^+ is observed at 1071 cm^{-1}. The intense peak position is consistent with the ring breathing mode of the oxidized nicotinamide ring for NAD^+ at 1032 cm^{-1},[32,33] considering the influence of the lipid membrane and ubiquinone molecules at the gold mesh electrode. Interestingly, the SERS bands changed significantly with variation in the applied voltage to −0.50 V, as shown in Figure 2, curve b. Two main features can be highlighted from the spectrum curve b. First, the strong diagnostic peaks at 1180 cm^{-1} for NADH,[33,34] which must have a significant contribution from a reduced nicotinamide ring mode in NADH. Second, though the overall shape of the Raman spectra is conserved, some subtle changes occur, suggesting the formation of different electrochemical-dependent NADH/NAD^+ species. The new peaks indicate that the NAD^+ molecules are transformed to NADH at sufficiently negative potentials. After applying an oxidizing potential of +0.50 V, the diagnostic NADH peak at 1180 cm^{-1} disappears and the characteristic band of 1071 cm^{-1} of the oxidized nicotinamide ring is observed, as shown in Figure 2, curve c. Clearly, Figure 2 shows that changes in the Raman peaks are consistent with NAD^+ molecules being electrochemically transformed to NADH species reversibly as a function of applied potential.

Practical methods for the redox cycling of NADH and NAD^+ are of significant interest in biocatalysis.[35,36] More importantly, enzymatically active NADH/NAD^+ should be regenerated to allow enzymes to continue their turnover because hundreds of dehydrogenase enzymes rely on the NADH/NAD^+ coenzyme couple in biological systems.[17] However, direct electrochemical NADH oxidation at a bare electrode surface does not permit regeneration of the biologically active NAD^+. Here, we performed enzymatic experiments on the $\mathbf{Q_5S}$-HBM on a larger-scale gold mesh electrode in a solution containing NADH dispersed in PBS, such that absorbance changes in solution could be monitored by UV−vis spectroscopy. As shown in Figure S29a (SI), the UV−vis characteristic absorption peak of NADH at 340 nm disappears slowly at an applied potential of ∼0.50 V vs Ag/AgCl. Alcohol dehydrogenase (ADH) catalyzes the oxidation of ethanol to acetaldehyde in the presence of NAD^+, which is reduced to NADH. To confirm that the NAD^+ produced electrochemically was active in a biological system, ADH and ethanol were added to the solution. As shown in Figure S29b (SI), the absorption peak at 340 nm gradually increases, demonstrating that the electrochemically produced NAD^+ can be used enzymatically to drive the conversion of ethanol to acetaldehyde.

In conclusion, we synthesized three ubiquinone-terminated disulfides with different alkyl spacers to form SAMs on gold electrodes. Biomimetic lipid bilayer membranes were then formed on the SAMs that contained embedded NAD^+ and NADH. Importantly, we have shown that reversible interconversion between NADH and NAD^+ could occur at a low overpotential when both ubiquinone, as a redox mediator, and NADH/NAD^+ were embedded in a lipid bilayer. Further evidence for the reversible interconversion NADH/NAD^+ was obtained by *in situ* SERS, and spectroelectrochemical UV−vis experiments confirmed that the electrochemical NADH oxidation at the ubiquinone HBM allows for the regeneration of biologically active NAD^+. Furthermore, this biomimetic membrane system could be useful as a platform to examine several biologically relevant electroactive molecules in lipid bilayer membranes.

■ ASSOCIATED CONTENT

Supporting Information. Experimental details. This material is available free of charge via the Internet at http://pubs.acs.org.

AUTHOR INFORMATION

Corresponding Author
ytlong@ecust.edu.cn

ACKNOWLEDGMENT

This research was supported by the Natural Science Foundation of China (Grant No. 91027035, 20933007), the Fundamental Research Funds for the Central Universities (Grant No. WK1013002) and the open research fund from Key Laboratory of Analytical Chemistry for Life Science of Nanjing University. Y.T.L. is supported by The Program for Professor of Special Appointment (Eastern Scholar) at Shanghai Institutions of Higher Learning.

REFERENCES

(1) Sazanov, L. A.; Hinchliffe, P. *Science* **2006**, *311*, 1430–1436.
(2) Sherwood, S.; Hirst, J. *Biochem. J.* **2006**, *400*, 541–550.
(3) Rhoten, M. C.; Hawkridge, F. M.; Wilczek, J. *J. Electroanal. Chem.* **2002**, *535*, 97–106.
(4) Suraniti, E.; Tumolo, T.; Baptista, M. S.; Livache, T.; Calemczuk, R. *Langmuir* **2007**, *23*, 6835–6842.
(5) Favero, G.; Campanella, L.; Cavallo, S.; D'Annibale, A.; Perrella, M.; Mattei, E.; Ferri, T. *J. Am. Chem. Soc.* **2005**, *127*, 8103–8111.
(6) Devadoss, A.; Burgess, J. D. *J. Am. Chem. Soc.* **2004**, *126*, 10214–10215.
(7) Burgess, J. D.; Rhoten, M. C.; Hawkridge, F. M. *Langmuir* **1998**, *14*, 2467–2475.
(8) Plant, A. L. *Langmuir* **1999**, *15*, 5128–5135.
(9) Peng, Z. Q.; Tang, J. L.; Han, X. J.; Wang, E. K.; Dong, S. J. *Langmuir* **2002**, *18*, 4834–4839.
(10) Anderson, N. A.; Richter, L. J.; Stephenson, J. C.; Briggman, K. A. *J. Am. Chem. Soc.* **2007**, *129*, 2094–2100.
(11) Twardowski, M.; Nuzzo, R. G. *Langmuir* **2004**, *20*, 175–180.
(12) Dominska, M.; Krysinski, P.; Blanchard, G. J. *Langmuir* **2008**, *24*, 8785–8793.
(13) Hosseini, A.; Collman, J. P.; Devadoss, A.; Williams, G. Y.; Barile, C. J.; Eberspacher, T. A. *Langmuir* **2010**, *26*, 17674–17678.
(14) Yang, L. C.; Calingasan, N. Y.; Wille, E. J.; Cormier, K.; Smith, K.; Ferrante, R. J.; Flint Bea, M. *J. Neurochem.* **2009**, *109*, 1427–1439.
(15) Jonassen, T.; Larsen, P. L.; Clarke, C. F. *Proc. Natl. Acad. Sci. U.S.A.* **2001**, *98*, 421–426.
(16) Yuasa, J.; Yamada, S.; Fukuzumi, S. *Angew. Chem., Int. Ed.* **2008**, *47*, 1068–1071.
(17) Gorton, L.; Dominguez, E. Electrochemistry of NAD(P)$^+$/NAD(P)H. In *Encyclopedia of Electrochemistry*; Wilson, G. S., Ed.; Wiley-VCH Verlag GmbH & Co.: Weinheim, 2002; Vol. 9, pp 67−143, 10.1002/9783527610426.bard090004.
(18) Antiochia, R.; Lavagnini, I.; Pastore, P.; Magno, F. *Bioelectrochemistry* **2004**, *64*, 157–163.
(19) Carlson, B. W.; Miller, L. L. *J. Am. Chem. Soc.* **1985**, *107*, 479–485.
(20) Antiochia, R.; Gallina, A.; Lavagnini, I.; Magno, F. *Electroanalysis* **2002**, *14*, 1256–1261.
(21) Wooten, M.; Gorski, W. *Anal. Chem.* **2010**, *82*, 1299–1304.
(22) Kitani, A.; Miller, L. L. *J. Am. Chem. Soc.* **1981**, *103*, 3595–3597.
(23) Zu, Y. B.; Shannon, R. J.; Hirst, J. *J. Am. Chem. Soc.* **2003**, *125*, 6020–6021.
(24) Qin, L. X.; Ma, W.; Li, D. W.; Li, Y.; Chen, X. Y.; Kraatz, H. B.; James, T. D.; Long, Y. T. *Chem.—Eur. J.* **2011**, *17*, 5262–5271.
(25) Daza Millone, M. A.; Vela, M. E.; Salvarezza, R. C.; Creczynski-Pasa, T. B.; Tognalli, N. G.; Fainstein, A. *ChemPhysChem* **2009**, *10*, 1927–1933.
(26) Marchal, D.; Pantigny, J.; Laval, J. M.; Moiroux, J.; Bourdillon, C. *Biochemistry* **2001**, *40*, 1248–1256.
(27) Hong, H. G.; Park, W. *Langmuir* **2001**, *17*, 2485–2492.
(28) Abhayawardhana, A. D.; Sutherland, T. C. *J. Electroanal. Chem.* **2011**, *653*, 50–55.
(29) Dieringer, J. A.; Lettan, R. B., II; Scheidt, K. A.; Van Duyne, R. P. *J. Am. Chem. Soc.* **2007**, *129*, 16249–16256.
(30) Ortiz, R. P.; Delgado, M. C. R.; Casado, J.; Hernández, V.; Kim, O.; Woo, H. Y.; López Navarrete, J. T. *J. Am. Chem. Soc.* **2004**, *126*, 13363–13376.
(31) Cortés, E.; Etchegoin, P. G.; Le Ru, E. C.; Fainstein, A.; Vela, M. E.; Salvarezza, R. C. *Anal. Chem.* **2010**, *82*, 6919–6925.
(32) Rinia, H. A.; Bonn, M.; Müller, M. *J. Phys. Chem. B* **2006**, *110*, 4472–4479.
(33) Chen, S. P.; Hosten, C. M.; Vivoni, A.; Birke, R. L.; Lombardi, J. R. *Langmuir* **2002**, *18*, 9888–9900.
(34) Siiman, O.; Rivellini, R.; Pate1, R. *Inorg. Chem.* **1988**, *27*, 3940–3949.
(35) Gebicki, J.; Marcinek, A.; Zielonka, J. *Acc. Chem. Res.* **2004**, *37*, 379–386.
(36) Yoon, S. K.; Choban, E. R.; Kan, C.; Tzedakis, T.; Kenis, P. J. A. *J. Am. Chem. Soc.* **2005**, *127*, 10466–10467.